Hole Quality Assessment in Drilling of Glass Microballoon/Epoxy Syntactic Foams

H. S. Ashrith, Mrityunjay Doddamani, Vinayak Gaitonde & Nikhil Gupta

JOM
The Journal of The Minerals, Metals & Materials Society (TMS)

ISSN 1047-4838
Volume 70
Number 7

JOM (2018) 70:1289-1294
DOI 10.1007/s11837-018-2925-x

Springer

JOM, Vol. 70, No. 7, 2018
https://doi.org/10.1007/s11837-018-2925-x

Hole Quality Assessment in Drilling of Glass Microballoon/ Epoxy Syntactic Foams

H.S. ASHRITH,[1] MRITYUNJAY DODDAMANI,[1,4] VINAYAK GAITONDE,[2] and NIKHIL GUPTA[3]

1.—Advanced Manufacturing Laboratory, Department of Mechanical Engineering, National Institute of Technology Karnataka, Surathkal, India. 2.—Department of Mechanical Engineering, BVB College of Engineering and Technology, Hubli, Karnataka, India. 3.—Composite Materials and Mechanics Laboratory, Mechanical and Aerospace Engineering Department, Tandon School of Engineering, New York University, Brooklyn, NY 11201, USA. 4.—e-mail: mrdoddamani@nitk.edu.in

Syntactic foams reinforced with glass microballoons are used as alternatives for conventional materials in structural application of aircrafts and automobiles due to their unique properties such as light weight, high compressive strength, and low moisture absorption. Drilling is the most commonly used process of making holes for assembling structural components. In the present investigation, grey relation analysis (GRA) is used to optimize cutting speed, feed, drill diameter, and filler content to minimize cylindricity, circularity error, and damage factor. Experiments based on full factorial design are conducted using a vertical computer numerical control machine and tungsten carbide twist drills. GRA reveals that a combination of lower cutting speed, filler content, and drill diameter produces a good quality hole at optimum intermediate feed in drilling syntactic foams composites. GRA also shows that the drill diameter has a significant effect on the hole quality. Furthermore, damage on the hole exit side is analyzed using a scanning electron microscope.

List of symbols

CYL	Cylindricity (mm)
$C_{\text{e-Exit}}$	Circularity error at exit (mm)
$F_{\text{d-Exit}}$	Damage factor at exit
v	Cutting speed (m/min)
f	Feed (mm/rev)
R	Filler content (volume %)
D	Drill diameter (mm)
$D_{\max}$	Maximum hole diameter (mm)
m	Total number of experiments
n	Total number of parameters
$X_i^o(k)$	Original data sequence
$X_i^*(k)$	Preprocessed data sequence
$\xi_i(k)$	Grey relation coefficient
Δ_{oi}	Deviation sequence
$X_o^*(k)$	Reference sequence
ζ	Identification coefficient
γ_i	Grey relation grade

INTRODUCTION

Syntactic foams are closed-cell particulate composites wherein hollow particles are dispersed in a matrix resin.[1–5] They are used in the marine, aerospace, automobile, sports equipment, and furniture industries due to their light weight combined with high compression strength and low moisture absorption.[6] In the aerospace and automobile industries, drilling is a widely used machining process for assembly of structural components.[7] Machining of syntactic foam is quite different from that of conventional materials as the tool has to pass alternately through the matrix, abrasive fillers, and air pockets, which offer variable resistance and significantly affect the hole quality. Hence, drilling behavior needs thorough understanding for syntactic foams.

Drilling of glass fiber-reinforced composites has been studied in detail. The effects of speed, feed, drill diameter, and fiber volume fraction on machinability characteristics, namely, thrust force, torque, surface roughness, and specific cutting coefficient, have been reported.[8–10] Results reveal that cutting speed has a negligible effect on thrust force, whereas the hole surface roughness is highly influenced by cutting speed, feed, and drill diameter. Feed is seen to be governing the specific cutting coefficient. The influence of cutting speed, feed, and drill geometry are analyzed in drilling of unreinforced and reinforced polyamides.[11,12] Results show that reinforced polyamide provides better

(Published online May 21, 2018)

machinability. Speed and feed in drilling carbon fiber-reinforced polymer (CFRP) composites are optimized using genetic algorithm,[13] and it is found that feed has a significant effect on thrust force, hole diameter, and delamination. Circularity of drilled holes is highly influenced by cutting speed. It is found that circularity decreases with an increase in cutting speed, while it remains almost constant for increase in feeds. Best results were obtained at a high cutting speed of 20,000 rpm for this material, suggesting the need for optimizing the cutting speed. Response surface methodology (RSM) models are used to analyze the effects of speed, feed, and point angle on delamination in drilling of CFRP.[14] Parametric analysis reveals that delamination in CFRP drilling can be minimized by choosing a higher cutting speed, lower feed, and point angle. The effects of cutting speed and constituent materials are analyzed in CFRP drilling.[15] The study found that the matrix material has a significant effect on thrust force and torque generated during drilling. Reinforcement type and cutting speed has a negligible effect on thrust force, whereas torque is governed by cutting speed.

RSM with single response optimization is widely used in drilling studies. A single setting of process parameters may be optimal for single quality characteristic, but the same settings may yield detrimental results for other quality features.[16] Therefore multiobjective optimization may be the solution to optimize multiresponses simultaneously like in grey relation analysis (GRA).[17] GRA has successfully been implemented in the past for process parameter optimization in the drilling process.[17–19]

Quantitative assessment of cylindricity and circularity error along with damage factor assessment are presented for glass microballoon (GMB)/epoxy syntactic foams. Furthermore, based on the experimental results, the process parameter (v, f, R and D) optimization using GRA is carried out to propose best hole quality parameters based on CYL, $C_{\text{e-Exit}}$, and $F_{\text{d-Exit}}$.

MATERIALS AND METHOD

Constituent Materials

Epoxy resin (LAPOX L-12) with polyamine hardener (K-6) procured from Atul Ltd., Valsad, Gujarat, India, is the matrix system used for sample fabrication. GMBs used as filler with an average particle size of 45 μm and true particle density of 350 kg/m^3 are procured from Trelleborg Offshore, Boston, MA.

Sample Preparation

Syntactic foams were fabricated by dispersing 20, 40, and 60 by vol.% GMBs in epoxy matrix to cover a wide range of material compositions.[1,20] GMBs were stirred slowly in epoxy resin at room temperature to obtain homogeneous slurry. Hardener by 10 wt.% was added to the slurry and stirred for additional 5 min. The mixture was degassed (10 min) before pouring into the molds (ϕ 35 $\times$ 16 mm) coated with silicone-releasing agent. The samples were cured at room temperature for 24 h and post cured at 90°C for additional 2 h. Samples were coded with EZZ convention, where E and ZZ represent epoxy matrix and filler vol.%, respectively. Supplementary Fig. S-1 shows an as-cast freeze fractured micrograph of a representative E60 specimen showing uniform dispersion of GMBs in the matrix.

Planning of Experiments

Speed, feed, and drill diameter are significant parameters that influence cylindricity, circularity error, and damage factor[12,13,19] and are considered in the present work along with filler content. The levels of these process parameters are chosen based on the available literature[1,9,14,18,21,22] and are presented in supplementary Table S-I. Drilling-induced damage on the exit side is more severe than on the entry side;[10] hence, circularity error and damage factor on exit side of drilled hole along with cylindricity are considered to be responses in the present investigation. Based on full factorial design (FFD), 81 experiments with three replicates for each run are conducted (Table I).

Based on FFD, experiments are conducted on a vertical computer numerical control (CNC) machine (MAX MILL PLUS+, MTAB, Chennai, India) using coated solid tungsten carbide drill bits. A coordinate measuring machine (Evolution 20.12.10, METRIS, UK) is used to measure the cylindricity and circularity error of drilled holes. The damage factor is given by Ref. 23:

$$F_d = \frac{D_{\max}}{D} \tag{1}$$

Input parameters (I) and their levels (L) are coded as I_L. For example, v_{25} represents 25-m/min cutting speed.

Grey Relation Optimization

GRA provides an efficient solution to uncertainty, multi-input, and discrete data problems.[18,19] It involves the measurement of absolute values of data differences between the sequences. The steps involved for optimizing the process parameters are as follows:

Step 1 Data normalization/preprocessing

The experimental data of the responses (CYL, $C_{\text{e-Exit}}$ and $F_{\text{d-Exit}}$) to be used in GRA must be preprocessed to be in the range of 0–1 for comparison. The lower-the-better characteristic of grey relation is used for data normalization since the objective is to minimize the responses. The equation used to normalize the data is given by:[19]

Table I. Experimental plan and measured average values of responses

Process parameter			E20			E40			E60		
v	F	D	CYL	$C_{\text{e-Exit}}$	$F_{\text{d-Exit}}$	CYL	$C_{\text{e-Exit}}$	$F_{\text{d-Exit}}$	CYL	$C_{\text{e-Exit}}$	$F_{\text{d-Exit}}$
25	0.04	8	0.021	0.011	1.002	0.016	0.006	1.002	0.024	0.006	1.002
		12	0.025	0.002	1.006	0.028	0.021	1.005	0.023	0.009	1.004
		16	0.014	0.013	1.007	0.023	0.019	1.006	0.030	0.012	1.007
	0.08	8	0.012	0.005	1.002	0.012	0.008	1.004	0.018	0.006	1.003
		12	0.023	0.005	1.007	0.014	0.006	1.007	0.015	0.006	1.004
		16	0.045	0.039	1.007	0.047	0.020	1.008	0.037	0.019	1.007
	0.12	8	0.018	0.009	1.004	0.022	0.012	1.003	0.018	0.004	1.003
		12	0.021	0.007	1.007	0.014	0.004	1.005	0.008	0.005	1.005
		16	0.042	0.018	1.009	0.048	0.022	1.005	0.031	0.015	1.008
75	0.04	8	0.017	0.007	1.003	0.007	0.006	1.003	0.014	0.003	1.003
		12	0.014	0.014	1.007	0.012	0.005	1.007	0.029	0.019	1.006
		16	0.028	0.023	1.008	0.032	0.029	1.007	0.016	0.011	1.007
	0.08	8	0.023	0.007	1.003	0.018	0.010	1.002	0.019	0.009	1.004
		12	0.016	0.010	1.007	0.021	0.012	1.006	0.016	0.016	1.005
		16	0.027	0.010	1.008	0.025	0.025	1.009	0.035	0.026	1.008
	0.12	8	0.021	0.010	1.003	0.018	0.010	1.003	0.014	0.014	1.004
		12	0.021	0.010	1.007	0.016	0.008	1.008	0.015	0.014	1.007
		16	0.020	0.016	1.009	0.028	0.022	1.009	0.022	0.017	1.008
125	0.04	8	0.019	0.013	1.003	0.010	0.006	1.003	0.016	0.011	1.002
		12	0.019	0.018	1.007	0.015	0.008	1.006	0.019	0.017	1.006
		16	0.043	0.034	1.008	0.039	0.018	1.009	0.036	0.023	1.008
	0.08	8	0.013	0.012	1.003	0.012	0.007	1.003	0.013	0.007	1.003
		12	0.018	0.007	1.008	0.010	0.003	1.007	0.019	0.013	1.007
		16	0.033	0.027	1.008	0.045	0.028	1.010	0.032	0.012	1.008
	0.12	8	0.016	0.009	1.004	0.014	0.009	1.004	0.028	0.010	1.004
		12	0.023	0.013	1.007	0.027	0.012	1.007	0.024	0.014	1.008
		16	0.024	0.017	1.008	0.035	0.028	1.009	0.013	0.014	1.008

$$X_i^*(k) = \frac{\max X_i^o(k) - X_i^o(k)}{\max X_i^o(k) - \min X_i^o(k)} \quad (2)$$

where i = 1… m; k = 1… n.

Step 2 Grey relation coefficient and grades

The grey relation coefficient is calculated using:[19]

$$\xi_i(k) = \frac{\Delta_{\min} + \zeta\Delta_{\max}}{\Delta_{oi}(k) + \zeta\Delta_{\max}} \quad (3)$$

$$\Delta_{oi}(k) = \left\| X_o^*(k) - X_i^*(k) \right\| \quad (4)$$

$$\Delta_{\max}(k) = \max\max\left\| X_o^*(k) - X_i^*(k) \right\| \quad (5)$$

$$\Delta_{\min}(k) = \min\min\left\| X_o^*(k) - X_i^*(k) \right\| \quad (6)$$

ζ is the identification coefficient and ζ = 0.5 is generally used for analysis.[18] The grey relation grade is calculated by taking the averages of the grey relation coefficient. The grey relation grade is calculated by:

$$\gamma_i = \frac{1}{n}\sum_{k=1}^{n}\xi_i(k) \quad (7)$$

The grey relation grade along with the rank is presented in the results.

RESULTS AND DISCUSSION

Experimental Investigation

Experimentally measured values of the responses (CYL, $C_{\text{e-Exit}}$, and $F_{\text{d-Exit}}$) are presented in Table I. Figure 1 presents the main effect plots of the responses. CYL decreases with increasing cutting speed up to v_{75} while an increasing trend is observed with a further increase in cutting speed. Increasing cutting speed increases vibration of the cutting tool resulting in high CYL values.[24] Increasing feed and drill diameter increases CYL while a decreasing trend is observed with increasing filler content (Fig. 1a). At lower feeds, the tool moves slowly along the axis of the hole leading to lower CYL values.[25]

Figure 1b shows that $C_{\text{e-Exit}}$ increases with speed and drill diameter while it decreases with increasing feed and filler content. Increasing v causes a high surface distortion of the sample due to the increased interaction of the tool and the drilled wall, which increases the circularity error. Lower values of circularity errors are observed at higher feeds due

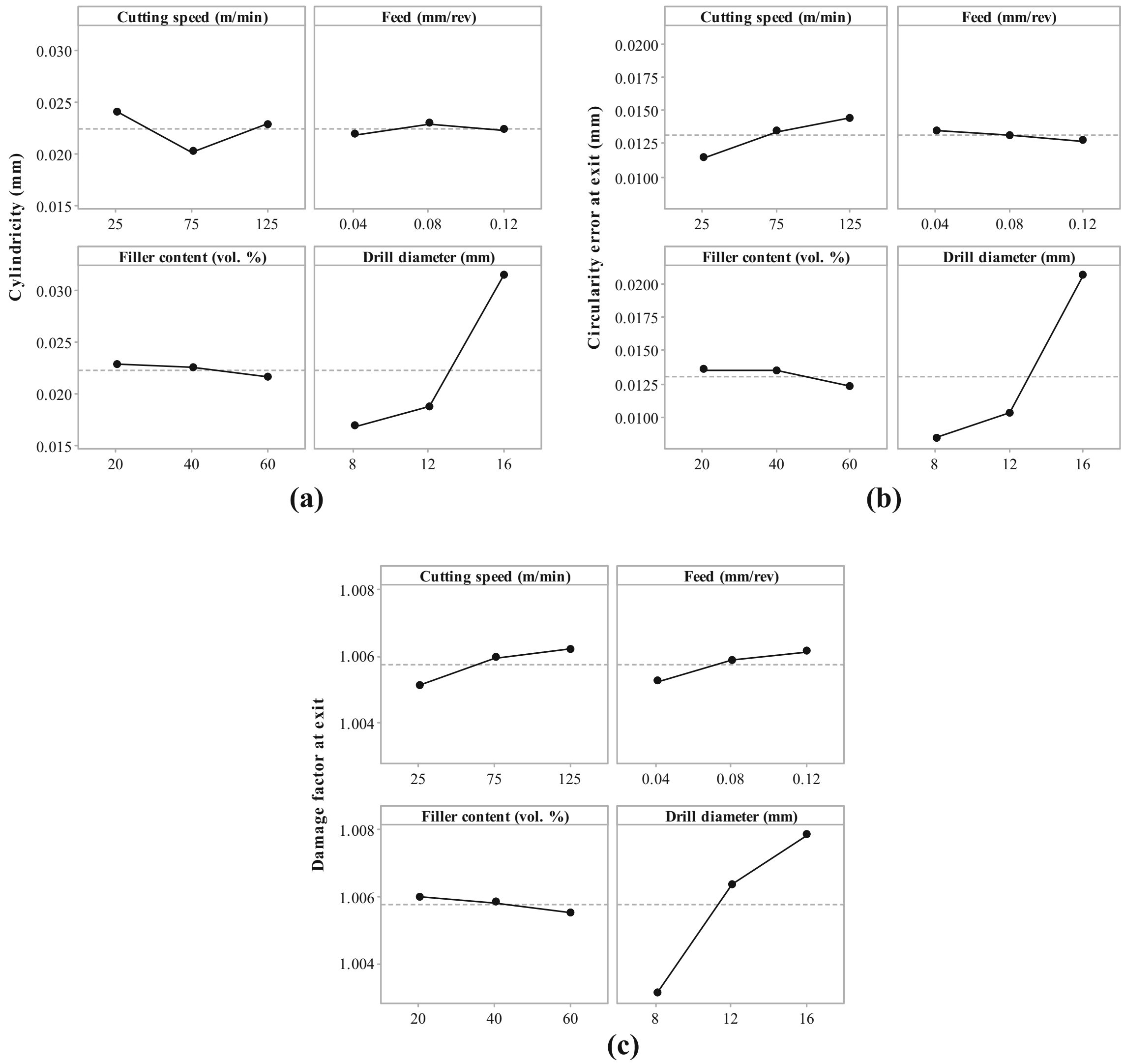

Fig. 1. Main effect plots for (a) cylindricity, (b) circularity error at exit, and (c) damage factor at exit showing the mean values.

to a reduced tool–workpiece interface temperature.[26] Increased thermal stability with increasing R[12] and lower cutting forces using smaller D leads to smaller circularity error values.[27] $F_{\text{d-Exit}}$ increases with increasing v, f, and D while it decreases with increasing R as shown in Fig. 1c. The damage factor is dependent on the thrust force developed during drilling process.[18] Increasing cutting speed increases thrust force results in higher values of damage factor. A higher value of damage factor is observed with increasing feed due to increased thrust force because of increased friction between tool and syntactic foam.[8] Thrust force increases with increasing drill diameter due to increased contact area resulting in higher damage factor values.[9] Supplementary Fig. S-2 shows a scanning electron micrograph of a part of a drilled hole. Comparing supplementary Fig. S-2a and S-2b, it is clear that the amount of damage occurred using D_8 is lesser than D_{16}. With increased GMBs, content thrust force decreases resulting in lower damage factor values.

It is observed from Fig. 1 that minimum CYL, $C_{\text{e-Exit}}$, and $F_{\text{d-Exit}}$ is observed at $v_{75}f_{0.04}R_{60}D_8$, $v_{25}f_{0.12}R_{60}D_8$, and $v_{25}f_{0.04}R_{60}D_8$, respectively. Intermediate cutting speed is required to reduce CYL whereas lower cutting speed is required to minimize $C_{\text{e-Exit}}$ and $F_{\text{d-Exit}}$. Similarly lower feed leads to reduced CYL and $F_{\text{d-Exit}}$ whereas higher feed is required to minimize $C_{\text{e-Exit}}$. The trade-off between cutting speed and feed for minimizing CYL, $C_{\text{e-Exit}}$, and $F_{\text{d-Exit}}$ leads to a multi-objective optimization problem. Hence, there is a need to optimize multiple process parameters using a suitable method. Therefore, in the present work, GRA is used to optimize the multiple process parameters (v, f, R, and D) to minimize CYL, $C_{\text{e-Exit}}$, and $F_{\text{d-Exit}}$ in drilling of syntactic foam composites.

Table II. Grey relation coefficient, grade, and rank

Process parameter			E20					E40					E60				
			ξ_i (K)					ξ_i (K)					ξ_i (K)				
v	f	D	CYL	$C_{e\text{-Exit}}$	$F_{d\text{-Exit}}$	γ_i	Rank	CYL	$C_{e\text{-Exit}}$	$F_{d\text{-Exit}}$	γ_i	Rank	CYL	$C_{e\text{-Exit}}$	$F_{d\text{-Exit}}$	γ_i	Rank
25	0.04	8	0.594	0.673	0.953	0.740	16	0.695	0.822	0.910	0.809	5	0.547	0.822	0.910	0.760	11
		12	0.532	1.000	0.498	0.677	29	0.494	0.493	0.553	0.513	59	0.562	0.725	0.708	0.665	32
		16	0.745	0.627	0.436	0.603	42	0.562	0.521	0.475	0.519	57	0.471	0.649	0.428	0.516	58
	0.08	8	0.804	0.860	0.968	0.877	1	0.804	0.755	0.691	0.750	15	0.651	0.822	0.781	0.751	14
		12	0.562	0.860	0.453	0.625	37	0.745	0.822	0.420	0.662	33	0.719	0.822	0.621	0.721	19
		16	0.350	0.333	0.428	0.370	80	0.339	0.507	0.394	0.413	76	0.406	0.521	0.416	0.448	68
	0.12	8	0.651	0.725	0.634	0.670	31	0.577	0.649	0.742	0.656	34	0.651	0.902	0.716	0.756	12
		12	0.594	0.787	0.440	0.607	40	0.745	0.902	0.553	0.733	18	0.953	0.860	0.573	0.796	6
		16	0.369	0.536	0.357	0.421	74	0.333	0.481	0.539	0.451	67	0.461	0.587	0.394	0.481	65
75	0.04	8	0.672	0.787	0.752	0.737	17	1.000	0.822	0.791	0.871	2	0.745	0.949	0.781	0.825	4
		12	0.745	0.607	0.440	0.597	44	0.804	0.860	0.436	0.700	22	0.482	0.521	0.515	0.506	61
		16	0.494	0.468	0.405	0.456	66	0.451	0.407	0.428	0.428	71	0.695	0.673	0.432	0.600	43
	0.08	8	0.562	0.787	0.725	0.691	26	0.651	0.698	0.938	0.762	10	0.631	0.725	0.676	0.677	28
		12	0.695	0.698	0.416	0.603	41	0.594	0.649	0.472	0.572	49	0.695	0.569	0.524	0.596	45
		16	0.506	0.698	0.399	0.535	53	0.532	0.446	0.349	0.442	70	0.423	0.435	0.381	0.413	77
	0.12	8	0.594	0.698	0.742	0.678	27	0.651	0.698	0.733	0.694	24	0.745	0.607	0.661	0.671	30
		12	0.594	0.698	0.432	0.575	48	0.695	0.755	0.394	0.615	38	0.719	0.607	0.434	0.587	46
		16	0.612	0.569	0.357	0.513	60	0.494	0.481	0.357	0.444	69	0.577	0.552	0.369	0.499	62
125	0.04	8	0.631	0.627	0.834	0.697	23	0.872	0.822	0.791	0.828	3	0.695	0.673	1.000	0.789	7
		12	0.631	0.536	0.428	0.532	54	0.719	0.755	0.462	0.646	35	0.631	0.552	0.506	0.563	50
		16	0.363	0.366	0.384	0.371	79	0.390	0.536	0.357	0.428	72	0.414	0.468	0.387	0.423	73
	0.08	8	0.774	0.649	0.725	0.716	20	0.804	0.787	0.733	0.775	9	0.774	0.787	0.801	0.787	8
		12	0.651	0.787	0.384	0.607	39	0.872	0.949	0.436	0.752	13	0.631	0.627	0.416	0.558	51
		16	0.441	0.425	0.379	0.415	75	0.350	0.416	0.333	0.366	81	0.451	0.649	0.372	0.490	64
	0.12	8	0.695	0.725	0.661	0.694	25	0.745	0.725	0.654	0.708	21	0.494	0.698	0.691	0.628	36
		12	0.562	0.627	0.422	0.537	52	0.506	0.649	0.412	0.522	55	0.547	0.607	0.405	0.519	56
		16	0.547	0.552	0.375	0.491	63	0.423	0.416	0.361	0.400	78	0.774	0.607	0.370	0.583	47

Grey Relation Optimization

Supplementary Table S-II presents the normalized data of the responses (CYL, $C_{e\text{-Exit}}$, and $F_{d\text{-Exit}}$) for comparison. Grey relation coefficients along with the grey relation grade and ranks are presented in Table II. From Table II, it is found that the highest grey relation grade (0.877) is observed at a combination of $v_{25}f_{0.08}R_{20}D_8$ that is the optimized condition. Performing machining at this optimized condition, i.e., using lower values of cutting speed, drill diameter, filler content, and intermediate feed, provides a good quality hole.

The influence of the process parameters on the machining performance needs to be analyzed to clearly determine the levels of process parameters at an optimized condition ($v_{25}f_{0.08}R_{20}D_8$). Average analysis is used to identify the process parameter influence, and the results are presented in supplementary Table S-III. A response table is calculated by taking the average of grey relation grades at a particular level. The delta in supplementary Table S-III is calculated by taking the difference between the maximum and minimum values of average grey relation grades at a particular level of process parameter. Grey relation grade graphs drawn using a response table are presented in supplementary Fig. S-3. The deviation of drill diameter from mean line is found to be more (supplementary Fig. S-3), indicating it has significant effect on CYL, $C_{e\text{-Exit}}$, and $F_{d\text{-Exit}}$. It is also observed from supplementary Table S-III that the drill diameter is the most influential process parameter on the hole quality. An ANOVA result for grey relation grade is presented in supplementary Table S-IV, which is used to find the percentage contribution of a significant process parameter. It is observed from supplementary Table S-IV that the drill diameter (73.12%) has a significant effect on CYL, $C_{e\text{-Exit}}$, and $F_{d\text{-Exit}}$ in drilling glass microballoon/epoxy syntactic foams followed by the interaction between drill diameter and feed. This investigation presents the guidelines for drilling quality holes in GMB/epoxy syntactic foams used for structural applications.

CONCLUSIONS

Syntactic foams were fabricated by dispersing 20, 40, and 60 vol.% of glass microballoons in epoxy matrix. Experiments were conducted based on FFD to evaluate the responses (CYL, $C_{e\text{-Exit}}$, and $F_{d\text{-Exit}}$), and the process parameters were optimized using grey relation analysis to minimize the responses. The following conclusions are drawn based on the analysis:

- Cylindricity of drilled holes is influenced by D.
- Drill diameter and its interaction with filler content has a significant effect on the $C_{\text{e-Exit}}$ of drilled holes.
- $F_{\text{d-Exit}}$ is strongly influenced by the drill diameter followed by cutting speed.
- Minimum CYL, $C_{\text{e-Exit}}$, and $F_{\text{d-Exit}}$ are obtained for a combination of $v_{75}f_{0.04}R_{60}D_8$, $v_{25}f_{0.12}R_{60}D_8$, and $v_{25}f_{0.04}R_{60}D_8$, respectively. The trade-off between v and f in minimizing responses leads to multi-objective optimization using GRA.
- According to GRA, CYL, $C_{\text{e-Exit}}$, and $F_{\text{d-Exit}}$ can be minimized at a combination of $v_{25}f_{0.08}R_{20}D_8$.
- At optimized conditions, the drill diameter has a significant effect on hole quality followed by its interaction with feed.
- SEM image shows more damage has appeared on larger diameter holes due to increased thrust force with increasing drill diameter.

The results can be extended to other types of syntactic foams containing a thermoset matrix reinforced with abrasive hollow particles such as silicon carbide and alumina.[1]

ACKNOWLEDGEMENTS

Department of Science and Technology Grant DST/TSG/AMT/2015/394/G is acknowledged by Mrityunjay Doddamani. Author Nikhil Gupta acknowledges the Office of Naval Research Grant N00014-10-1-0988. The authors thank the ME Department at NIT-K and MAE Department at NYU for providing facilities and support.

ELECTRONIC SUPPLEMENTARY MATERIAL

The online version of this article (https://doi.org/10.1007/s11837-018-2925-x) contains supplementary material, which is available to authorized users.

REFERENCES

1. N. Gupta, D. Pinisetty, and V.C. Shunmugasamy, *Reinforced Polymer Matrix Syntactic Foams: Effect of Nano and Micro-Scale Reinforcement* (New York: Springer, 2013).
2. M. Jayavardhan, B.B. Kumar, M. Doddamani, A.K. Singh, S.E. Zeltmann, and N. Gupta, *Compos. Part B Eng.* 130, 119 (2017).
3. A.K. Singh, B. Patil, N. Hoffmann, B. Saltonstall, M. Doddamani, and N. Gupta, *JOM* 70, 303 (2018).
4. A.K. Singh, B. Saltonstall, B. Patil, N. Hoffmann, M. Doddamani, and N. Gupta, *JOM* 70, 310 (2018).
5. M. Doddamani and S. Kulkarni, *Polym. Compos.* 32, 1541 (2011).
6. N. Gupta, S.E. Zeltmann, V.C. Shunmugasamy, and D. Pinisetty, *JOM* 66, 245 (2014).
7. C. Tsao, *Mater. Des.* 29, 1740 (2008).
8. S. Basavarajappa, A. Venkatesh, V. Gaitonde, and S. Karnik, *J. Thermoplast. Composite Mater.* 25, 363 (2012).
9. I. El-Sonbaty, U. Khashaba, and T. Machaly, *Compos. Struct.* 63, 329 (2004).
10. U. Khashaba, I. El-Sonbaty, A. Selmy, and A. Megahed, *Compos. A Appl. Sci. Manuf.* 41, 391 (2010).
11. V. Gaitonde, S. Karnik, J.C. Rubio, A. Abrão, A.E. Correia, and J.P. Davim, *J. Composite Mater.* 46, 2659 (2012).
12. V. Gaitonde, S. Karnik, J.C.C. Rubio, W. de Oliveira Leite, and J. Davim, *J. Composite Mater* 48, 21 (2014).
13. V. Krishnaraj, A. Prabukarthi, A. Ramanathan, N. Elanghovan, M.S. Kumar, R. Zitoune, and J. Davim, *Composites Part B Eng.* 43, 1791 (2012).
14. V. Gaitonde, S. Karnik, J.C. Rubio, A.E. Correia, A. Abrao, and J.P. Davim, *J. Mater. Process. Tech.* 203, 431 (2008).
15. J.L. Merino-Pérez, R. Royer, E. Merson, A. Lockwood, S. Ayvar-Soberanis, and M.B. Marshall, *Compos. Struct.* 140, 621 (2016).
16. Y. Kumar and H. Singh, *Procedia Mater. Sci.* 5, 2142 (2014).
17. J. Huang and Y. Liao, *Int. J. Production Res.* 41, 1244 (2003).
18. K. Palanikumar, *Measurement* 44, 2138 (2011).
19. S. Sheth and P. George, *Precis. Eng.* 45, 33 (2016).
20. S. Zeltmann, B. Chen, and N. Gupta, *Mater. Perform. Charact.* 6, 1 (2017).
21. S. Karnik and V. Gaitonde, *Int. J. Manufact. Technol.* 39, 439 (2008).
22. K. Palanikumar and R. Karthikeyan, *Mater. Des.* 28, 1584 (2007).
23. B. Ramesh, A. Elayaperumal, S. Satishkumar, A. Kumar, T. Jayakumar, and D. Dinakaran, *Arch. Civil Mech. Eng.* 16, 135 (2016).
24. E. Capello, *J. Mater. Process. Technol.* 148, 186 (2004).
25. A. Sultan, S. Sharif, and D. Kurniawan, *Procedia Manufact.* 2, 202 (2015).
26. J.C. Campos Rubio, A.M. Abrão, P. Eustaquio Faria, A.E. Correia, and J.P. Davim, *J. Composite Mater* 42, 1523 (2008).
27. K. Giasin and S. Ayvar-Soberanis, *Compos. Struct.* 159, 745 (2017).